Recent Advances in Single-carrier Frequency-domain Equalization and Distributed Antenna Network

F. Adachi, K. Takeda, T. Obara, T. Yamamoto, and H. Matsuda
Dept. of Electrical and Communication Engineering,
Graduate School of Engineering, Tohoku University
Sendai, Japan
adachi@ecei.tohoku.ac.jp

***Abstract*— In the future wireless communication systems, the broadband wireless technology which enables Giga-bps class data services is demanded. Broadband wireless channels become extremely frequency-selective and cause severe inter-symbol interference (ISI). Furthermore, the average received signal power changes in a random manner because of the shadowing and path losses according to the movement of a mobile terminal (MT). Accordingly, the transmission performance severely degrades. Development of some advanced equalization and networking is necessary to overcome the performance degradation. Among them, promising are the frequency-domain equalization (FDE) and distributed antenna network (DAN). The former takes advantage of channel frequency-selectivity to obtain the frequency-diversity gain. In DAN, a group of distributed antennas serve each user to mitigate the negative impact of shadowing and path losses. This article will introduce the recent advances in FDE and DAN for the broadband single-carrier (SC) transmissions.**

***Index Terms*—Single-carrier, frequency-domain equalization, distributed antenna, MIMO, signal detection**

I. INTRODUCTION

The future wireless communications systems are expected to offer a variety of broadband data services of close to or even above 1 Gbps [1]. However, for such broadband data services, channels become extremely frequency-selective and cause severe inter-symbol interference (ISI), thereby severely degrading the bit error rate (BER) performance [2]. Thus, the use of an advanced equalization technique is indispensable. In general, there are two types of signal transmission: multi-carrier (MC) and single-carrier (SC). An advantage of SC signal transmission over MC is its lower peak-to-average power ratio (PAPR). This lower PAPR property of SC is quite beneficial for the uplink (terminal-to-base) transmissions.

As for SC equalization, simple one-tap frequency-domain equalization (FDE) has been extensively studied [3-6]. While one-tap FDE is simple, it can exploit the channel frequency-selectivity to improve the BER performance. However, since one-tap FDE cannot completely remove the ISI, its performance improvement is limited. Recently, we proposed a new frequency-domain block signal detection that incorporates the idea of multi-input/multi-output (MIMO) signal detection into FDE to effectively suppress the ISI [7].

In addition to the ISI problem, the shadowing and distant-dependent path losses cause a severe power problem, in particular, for the broadband wireless systems since the transmit power is limited. The power problem is a crucial issue to tackle as well as the ISI problem in order to make the frequency and power efficient broadband wireless communication systems a reality. Distributed antenna system or network (DAS or DAN) [8-13] can solve the power problem. In DAN, many antennas are spatially distributed over a coverage area of each base station (BS). Some of distributed antennas can always be visible from a mobile terminal (MT) and they can cooperate to perform space diversity, beam forming, or spatial multiplexing. Since different antennas are located at different positions, DAN can exploit the random variations in the shadowing and path losses. We have been investigating the potential of DAN using maximal-ratio transmission (MRT) [13].

This article will introduce the recent advances in FDE and DAN for the broadband SC signal transmissions.

II. BROADBAND WIRELESS CHANNEL

There are several large obstacles between a BS and an MT and also many local scatterers (such as neighboring buildings) in the vicinity of the MT. The reflection of the signal by large obstacles creates the propagation paths with different time delays; each path is a cluster of irresolvable multipaths created by reflection or diffraction, by local scatterers, of the transmitted signal reaching the surroundings of the MT. Such a fading channel model is presented in Fig. 1.

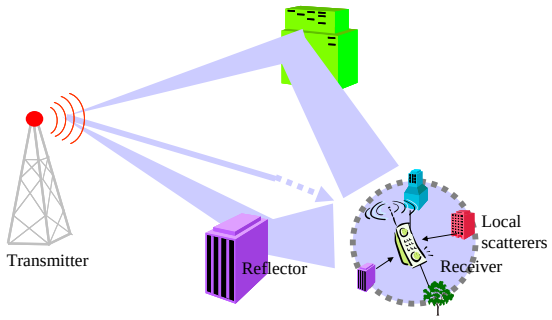

Fig. 1 Fading channel model.

The channel transfer function severely changes both in the frequency- and time-domains with the movement of an MT. However, for the broadband SC signal transmissions, the channel stays constant during the signal transmission; therefore, the time-selectivity can be neglected. Assuming a

symbol-spaced L–path channel, the channel impulse response $h(\tau)$ can be expressed as [14]

$$h(\tau)=\sum_{l=0}^{L-1}h_l\delta(\tau-\tau_l)\,, \qquad (1)$$

where h_l and τ_l are the complex-valued path gain with $E\left[\sum_{l=0}^{L-1}|h_l|^2\right]=1$ ($E[.]$ denotes the expectation operation) and the lth path time delay, respectively.

The channel transfer function (or the channel gain at frequency f) is the Fourier transform of $h(\tau)$ and is given by

$$H(f)=\sum_{l=0}^{L-1}h_l\exp(-j2\pi f\tau_l)\,. \qquad (2)$$

When $H(f)$ changes within the signal bandwidth, the channel is called the frequency-selective channel. A one shot observation of $H(f)$ is illustrated in Fig. 2. A frequency-selective channel having an L=16-path uniform power delay profile with $\mathrm{E}[|h_l|^2]=1/L$ and $\tau_l=l\times100$ ns (i.e., the l-th path length is $l\times30$ m) is assumed. The frequency-selective channel severely distorts the received SC signal spectrum and thus, the use of advanced equalization techniques is indispensable [2].

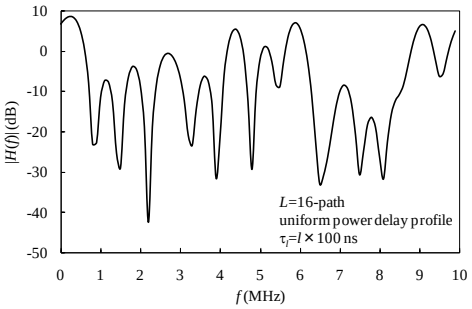

Fig. 2 Frequency-selective channel.

III. Channel Capacity of SC Signal Transmission

The channel capacity analysis for broadband SC transmissions is an interesting study topic. In [15], the achievable channel capacity of SC transmissions with FDE in a frequency-selective channel is theoretically examined and compared to that of orthogonal frequency division multiplexing (OFDM). It is shown that the OFDM with adaptive modulation provides always higher channel capacity than SC using one-tap FDE. However, below we will show that when block signal detection is utilized, broadband SC transmissions have a potential to achieve the same channel capacity as OFDM.

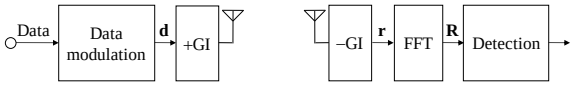

Fig. 3 SC signal transmission system model.

The SC signal transmission system model is illustrated in Fig. 3. A signal block $\mathbf{d}=[d(0),\cdots,d(t),\cdots,d(N_c-1)]^T$ of N_c data-modulated symbols is transmitted over a frequency-selective channel (in this paper, for the simplicity purpose, we omit the insertion and removal of cyclic prefix (CP)). The received signal block $\mathbf{r}=[r(0),\cdots,r(t),\cdots,r(N_c-1)]^T$ can be expressed in the matrix form as

$$\mathbf{r}=\sqrt{\frac{2E_s}{T_s}}\mathbf{H}\mathbf{d}+\mathbf{n}\,, \qquad (3)$$

where E_s and T_s are respectively the data-modulated symbol energy and length, $\mathbf{h}$ is the channel impulse response matrix given as

$$\mathbf{h}=\begin{bmatrix} h_0 & & & & h_{L-1} & \cdots & h_1 \\ h_1 & \ddots & & & & \ddots & \vdots \\ \vdots & \ddots & h_0 & & \mathbf{0} & & h_{L-1} \\ h_{L-1} & & h_1 & \ddots & & & \\ & \ddots & \vdots & \ddots & \ddots & & \\ & & h_{L-1} & & \ddots & h_0 & \\ & & & \ddots & & h_1 & \ddots \\ \mathbf{0} & & & & \ddots & \vdots & \ddots & h_0 \end{bmatrix}, \qquad (4)$$

and $\mathbf{n}=[n(0),\cdots,n(t),\cdots,n(N_c-1)]^T$ is the noise vector. The received signal block is transformed by an N_c-point fast Fourier transform (FFT) into the frequency-domain signal $\mathbf{R}=[R(0),\cdots,R(k),\cdots,R(N_c-1)]^T$ as

$$\mathbf{R}=\mathbf{F}\mathbf{r}=\sqrt{\frac{2E_s}{T_s}}\mathbf{H}\mathbf{F}\mathbf{d}+\mathbf{N}\,, \qquad (5)$$

where $\mathbf{H}=\mathbf{F}\mathbf{h}\mathbf{F}^{\mathrm{H}}$ and $\mathbf{N}=\mathbf{F}\mathbf{n}$ with $[.]^{\mathrm{H}}$ denoting the Hermitian transpose operation and $\mathbf{F}$ being an $N_c\times N_c$ FFT matrix given by

$$\mathbf{F}=\frac{1}{\sqrt{N_c}}\begin{bmatrix} 1 & 1 & \cdots & 1 \\ 1 & e^{-j2\pi\frac{1\times1}{N_c}} & \cdots & e^{-j2\pi\frac{1\times(N_c-1)}{N_c}} \\ \vdots & \vdots & \ddots & \vdots \\ 1 & e^{-j2\pi\frac{(N_c-1)\times1}{N_c}} & \cdots & e^{-j2\pi\frac{(N_c-1)\times(N_c-1)}{N_c}} \end{bmatrix}. \qquad (6)$$

$\mathbf{H}$ is the channel matrix, which is diagonal because of the circulant property of $\mathbf{h}$, and is given by

$$\mathbf{H} = \mathbf{F}\mathbf{h}\mathbf{F}^{\mathrm{H}} = \begin{bmatrix} H(0) & & & & \\ & \ddots & & \mathbf{0} & \\ & & H(k) & & \\ & \mathbf{0} & & \ddots & \\ & & & & H(N_c-1) \end{bmatrix}. \quad (7)$$

Equation (5) implies that the SC frequency-domain received signal has the same signal representation as an $N_c \times N_c$ MIMO multiplexing with channel matrix $\mathbf{HF}$ but with the reduced symbol rate by a factor of N_c. Following [16], the channel capacity C of SC frequency-domain block signal detection is given, from Eq. (5), as

$$\begin{aligned} C &= \frac{1}{N_c}\log_2 \det\left(\mathbf{I} + \frac{Es}{N_0}(\mathbf{HF})(\mathbf{HF})^H\right) \\ &= \frac{1}{N_c}\sum_{k=0}^{N_c-1}\log_2\left(1+\frac{E_s}{N_0}|H(k)|^2\right) \end{aligned}, \quad (8)$$

which is identical to the channel capacity of OFDM with N_c subcarriers [17].

IV. Frequency-Domain Block Signal Detection

Based on the fact that the SC frequency-domain received signal has the same signal representation as an $N_c \times N_c$ MIMO multiplexing, we proposed a new SC signal detection, called frequency-domain block signal detection [7]. The SC frequency-domain block signal detection incorporates the signal detection scheme developed for the MIMO multiplexing into FDE. The conceptual structure of SC transmission using frequency-domain block signal detection is illustrated in Fig. 4.

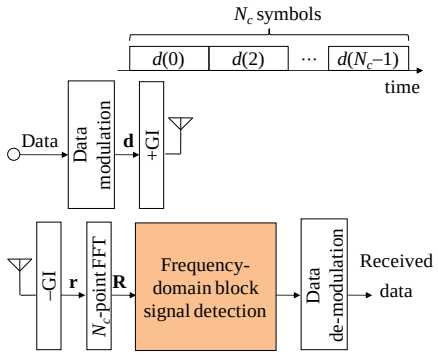

Fig. 4 Conceptual structure of SC transmission using frequency-domain block signal detection.

Among the well-known MIMO signal detection schemes, the Vertical-Bell Laboratories layered space-time architecture (V-BLAST) detection [18] and the maximum likelihood detection (MLD) employing QR decomposition/M-algorithm (QRM-MLD) [19] can be used. QRM-MLD is known to achieve the BER performance fairly close to MLD but with quite reduced complexity. The algorithms of V-BLAST detection and QRM-MLD are illustrated in Fig.5.

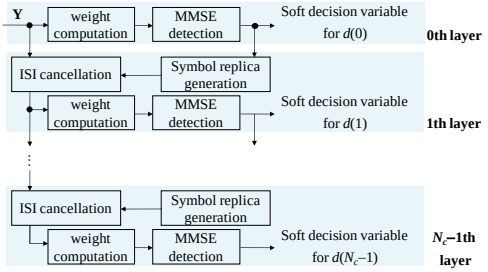

(a) V-BLAST detection

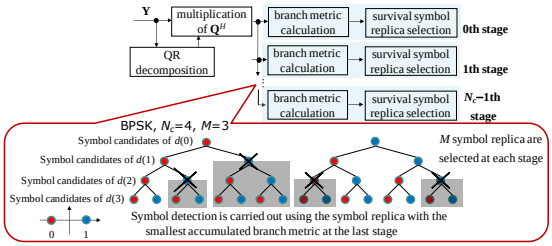

(b) QRM-MLD

Fig. 5 V-BLAST detection and QRM-MLD.

A. *Iterative V-BLAST detection*

The frequency-domain block signal detection using V-BLAST detection can achieve better BER performance than the conventional one-tap FDE based on the minimum mean square error criterion (MMSE-FDE).

The V-BLAST detection is composed of i) ordering, ii) ISI cancellation, and iii) signal detection. The transmitted symbol which has the highest signal-to-interference plus noise power ratio (SINR) among undetected symbols is detected by performing MMSE detection [20]. However, in the case of SC transmission, since the SINR is the same for all symbols, no ordering is necessary; the detection can be carried out simply from the first symbol (i.e., $d(0)$) in a block. The replica of the symbol, which has been just detected, is generated and is subtracted from the received signal (i.e., ISI cancellation). A new MMSE weight matrix for the next symbol to be detected is re-computed. Until all of the transmitted symbols are detected, the above symbol detection & ISI cancellation is repeated.

The V-BLAST detection cannot suppress the ISI sufficiently, in particular for those symbols which have been detected earlier. To further improve the BER performance, iterative detection can be applied [21]. After all of transmitted symbols are detected, the V-BLAST detection is carried out again. This is repeated a sufficient number of times. Below, the signal detection at the nth layer (n=0~N_c–1) in the ith iteration stage is presented (assuming that the symbols with n'=0~n–1 have been detected.

1) ISI cancellation

The frequency-domain received signal vector $\tilde{\mathbf{R}}^{(i,n)}$ at the nth layer in the ith iteration stage is given by

$$\tilde{\mathbf{R}}^{(i,n)} = \mathbf{R} - \sqrt{\frac{2E_s}{T_s}}\overline{\mathbf{H}}\hat{\mathbf{d}}^{(i,n)}, \quad (9)$$

where $\overline{\mathbf{H}} = \mathbf{HF} = [\overline{\mathbf{H}}_0, \cdots, \overline{\mathbf{H}}_n, \cdots, \overline{\mathbf{H}}_{N_c-1}]$ and $\hat{\mathbf{d}}^{(i,n)} = [\hat{d}^{(i)}(0), \cdots, \hat{d}^{(i)}(n-1), 0, \hat{d}^{(i-1)}(n+1), \cdots, \hat{d}^{(i-1)}(N_c-1)]$ $\hat{d}^{(i-1)}(N_c-1)]^T$ is the soft decision replica vector. The soft decision variable $\hat{d}^{(i)}(n)$ associated with $d(n)$ is generated using a sequence of log likelihood ratios (LLRs). Since the symbols with indices n'=0~(n–1) have already been detected, their replicas are generated using LLRs of the present iteration stage. The symbols with indices n'=n~(N_c–1) are undetected and hence, their replicas are generated using LLRs of the previous iteration stage.

2)MMSE detection

The ISI still remains after ISI cancellation and therefore, the MMSE weight matrix needs to be updated taking into account the residual ISI at each layer in each iteration stage. The MMSE weight matrix updating proposed in [22] can be applied.

The MMSE weight matrix taking into account the residual ISI at the nth layer in the ith iteration stage is given by

$$\mathbf{W}^{(i,n)} = \overline{\mathbf{H}}_n^H \left[\overline{\mathbf{H}} \boldsymbol{\rho}^{(i,n)} \overline{\mathbf{H}}^H + \left(\frac{E_s}{N_0} \right)^{-1} \mathbf{I}_{N_c} \right]^{-1}, \qquad (10)$$

where $\boldsymbol{\rho}^{(i,n)} = \mathrm{diag}[\rho_0^{(i)}, \cdots, \rho_n^{(i)}, \cdots, \rho_{N_c-1}^{(i)}]$ with $\rho_n^{(i)} = E[|\, d(n) - \hat{d}^{(i)}(n)\,|^2]$ representing the extent to which the residual ISI remains on the nth symbol [23] By setting $\rho_n^{(i)} = 1$, the nth symbol is detected. When i=0, the symbols with n'=n~(N_c–1) are undetected and hence, $\rho_{n'}^{(i)}$ is replaced by 1. After ISI cancellation using soft replicas as shown by Eq. (9), MMSE detection on the nth symbol is performed by multiplying the frequency-domain received signal vector $\tilde{\mathbf{R}}^{(i,n)}$ by 1×N_c MMSE weight matrix $\mathbf{W}^{(i,n)}$ as

$$\hat{d}^{(i)}(n) = \mathbf{W}^{(i,n)} \tilde{\mathbf{R}}^{(i,n)}. \qquad (11)$$

B. QRM-MLD

In the case of SC transmissions, all symbols have the same SINR and hence, no ordering is necessary; signal detection can be carried out simply from the last symbol $d(N_c-1)$. The channel matrix $\overline{\mathbf{H}}$ is decomposed by using the QR decomposition as

$$\overline{\mathbf{H}} = \mathbf{QU}, \qquad (12)$$

where $\mathbf{Q}$ is an N_c×N_c unitary matrix (i.e., $\mathbf{Q}^H\mathbf{Q}$=$\mathbf{I}$ with $\mathbf{I}$ representing the identity matrix) and $\mathbf{U}$ is an N_c×N_c upper triangular matrix given by

$$\mathbf{U} = \mathbf{Q}^H \overline{\mathbf{H}} = \begin{bmatrix} U_{0,0} & U_{0,1} & \cdots & U_{0,N_c-1} \\ & U_{1,1} & \cdots & U_{1,N_c-1} \\ & & \ddots & \vdots \\ \mathbf{0} & & & U_{N_c-1,N_c-1} \end{bmatrix}. \qquad (13)$$

The transformed frequency-domain received signal $\hat{\mathbf{R}}$ is obtained as

$$\hat{\mathbf{R}} = \mathbf{Q}^H \mathbf{R} = \sqrt{\frac{2E_s}{T_s}} \mathbf{Ud} + \mathbf{Q}^H \mathbf{N}. \qquad (14)$$

The M-algorithm [24] is composed of N_c stages, each corresponding to each symbol in a block. In each stage, the branch metric defined as the squared Euclidian distance from $\hat{\mathbf{R}}$ is computed for all candidate symbols connected to each of M surviving symbols in the previous stage and then, only a total of M symbols having the smallest accumulated branch metrics are selected as the surviving symbols in the present stage and others are discarded. This process is repeated until the last stage. Finally, the symbol which has the smallest accumulated branch metric is chosen and a sequence of N_c detected symbols is obtained by tracing back the surviving symbols until the first stage.

C. BER Performance

We assume a block transmission of N_c=64 symbols. The channel is assumed to be a frequency-selective block Rayleigh fading channel having symbol-spaced L=16-path uniform power delay profile. Ideal channel estimation is assumed. The average BER performances of SC block signal detection using iterative V-BLAST detection and QRM-MLD are compared in Fig. 6 as a function of the average received signal energy per bit-to-noise power spectrum density ratio E_b/N_0. For QRM-MLD, three cases of the number M of surviving symbols in each stage are plotted, i.e., M=16, 64, and 256. Also plotted are the BER performances achievable by the one-tap MMSE-FDE and the theoretical lower bound.

It can be seen from Fig. 6 that as the number i of iterations increases, iterative V-BLAST detection improves the BER performance. This is because the residual ISI is effectively reduced by using the MMSE weight taking into account the residual ISI and because the error propagation can be prevented by soft ISI cancellation. It can be seen the use of 2 iterations (i=2) provides sufficient performance improvement. For QPSK (16QAM), the E_b/N_0 gap from the theoretical lower bound for the average BER=10^{-4} is reduced by 1.5 (3.2) dB when i=2. When QPSK is used, both iterative V-BLAST detection and QRM-MLD provide almost identical BER performance. However, when 16QAM is used, QRM-MLD with either M=64 or 256 provides better performance than iterative V-BLAST detection.

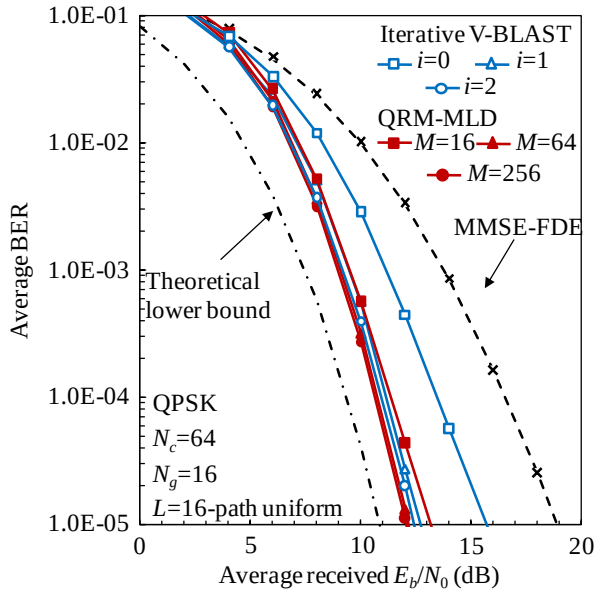

(a) QPSK

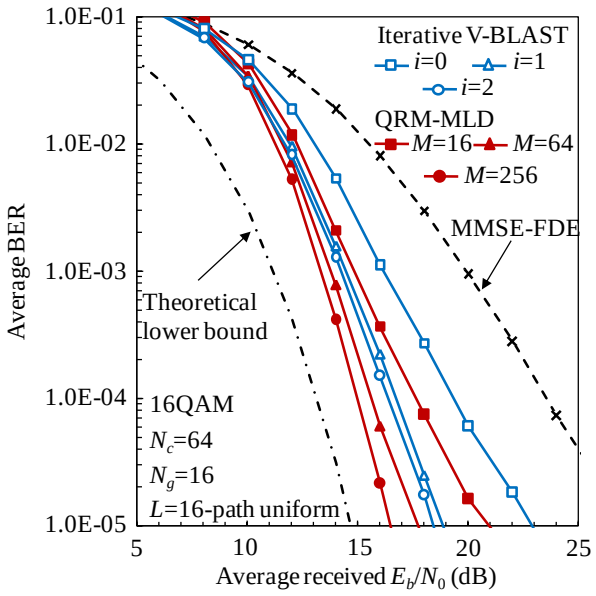

(b) 16 QAM

Fig. 6 BER performance of SC block signal detection.

V. OVERSAMPLING MMSE-FDE

In most of spectrum-efficient wireless communication systems, a square-root Nyquist filter is used at the transmitter and receiver to limit the signal bandwidth while maximizing the received signal-to-noise power ratio (SNR). However, when timing offset exists between the transmitter and receiver, the spectrum of the received signal sequence sampled at symbol rate is distorted and hence, the BER performance degrades as the filter roll-off factor α increases. This is because adjacent frequency-shifted spectra (which are the copies of the original spectrum), which are given different phase rotations due to the timing offset, overlap when $\alpha \neq 0$.

To solve the timing offset problem, recently, we proposed an oversampling MMSE-FDE [25]. Its receiver structure is illustrated in Fig. 7. First, the received signal is oversampled at 2 times higher rate than the symbol rate to prevent the spectrum overlapping. Then, the received signal sample sequence is transformed by a $2N_c$-sample FFT into the frequency domain signal $\{R(k);k=-N_c\sim N_c-1\}$. $R(k)$ can be expressed as

$$R(k)=\sqrt{\frac{2E_s}{T_s}}\tilde{H}(k,\Delta)S(k)+\mathrm{N}(k)+\Pi(k), \qquad (15)$$

where $\tilde{H}(k,\Delta)$ is the overall transfer function of the transmit/receive filters plus propagation channel including the phase rotation due to the timing offset Δ and $S(k)$, $\mathrm{N}(k)$, and $\Pi(k)$ are the signal, the inter-block interference (IBI), and the noise, respectively.

One-tap MMSE-FDE is applied to simultaneously compensate both the phase rotation due to the timing offset and the spectrum distortion due to the channel frequency-selectivity as

$$\hat{R}(k)=R(k)W(k) \qquad (16)$$

where $W(k)$ is the MMSE-FDE weight given as

$$W(k)=\frac{\tilde{H}^*(k,\Delta)\Phi(k)}{\left|\tilde{H}(k,\Delta)\right|^2+\Lambda^{-1}(k,\Delta)} \qquad (17)$$

with $\Phi(k)$ and $\Lambda(k,\Delta)$ being the overall transfer function of the transmit/receive filters and the signal-to-IBI plus noise power ratio (SINR), respectively.

After MMSE-FDE, the spectrum combing (or the frequency-domain down-sampling) is performed (see Fig. 8) to restore the ISI-free condition as

$$\tilde{R}(k)=\hat{R}(k-N_c)+\hat{R}(k)+\hat{R}(k+N_c) \qquad (18)$$

for $k=-N_c/2\sim N_c/2-1$.

It is seen from Fig. 9 that the proposed oversampling MMSE-FDE provides a good BER performance irrespective of the value of α in the presence of the timing offset.

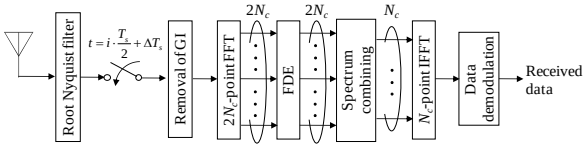

Fig. 7 Oversampling MMSE-FDE receiver.

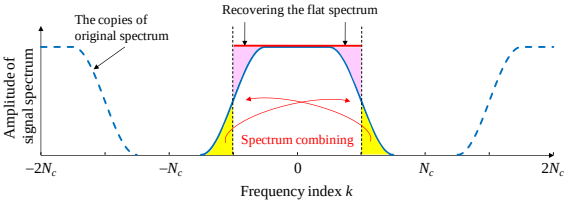

Fig. 8 Spectrum combining after one-tap MMSE-FDE.

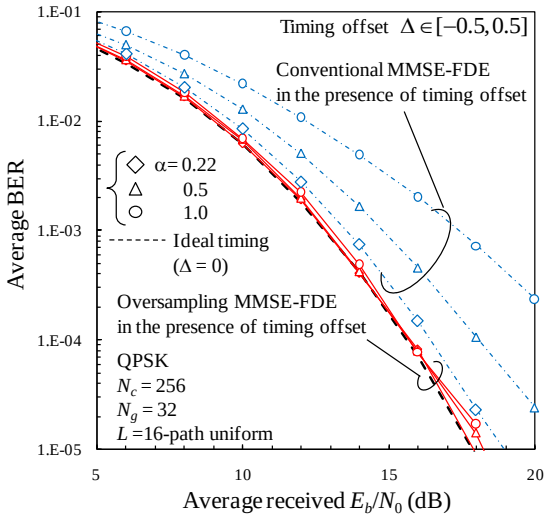

Fig. 9 BER performance in the presence of timing offset.

VI. Distributed Antenna Network

In DAN, many antennas are spatially distributed around each BS so that with a high probability, some antennas can always be visible from an MT. Antennas are connected to a BS by means of optical fiber or wireless links, as illustrated in Fig. 10. Many antennas cooperatively act as space diversity branches for improving the transmission quality. The distributed antenna diversity can mitigate the received signal power problem caused by distance-dependent path loss and shadowing loss as well as the frequency-selective fading.

One of promising distributed antenna diversity for DAN downlink is MRT [26]. In a frequency-selective channel, MRT is incorporated into the transmit FDE. This is called MRT-FDE. As seen in Fig. 11, the signal block is simultaneously transmitted from N_t different antennas close to an MT after multiplying MRT-FDE weight $\{W_m(k);\ k=0\sim N_c-1\}$, $m=0\sim N_t-1$, so that the same frequency components transmitted from different antennas are coherently combined at the MT, where N_t is the number of distributed antennas involved in MRT-FDE.

The signal block $\mathbf{d}$ is transmitted from N_t different antennas after performing MRT-FDE. The transmitted signal can be expressed using the matrix form as

$$\begin{aligned}\mathbf{s} &= [\mathbf{s}_0, \cdots, \mathbf{s}_m, \cdots, \mathbf{s}_{N_t-1}]^T \\ &= [\mathbf{F}^H \mathbf{W}_0 \mathbf{D}, \cdots, \mathbf{F}^H \mathbf{W}_m \mathbf{D}, \cdots, \mathbf{F}^H \mathbf{W}_{N_t-1} \mathbf{D}]^T\end{aligned}. \quad (19)$$

where $\mathbf{D} = [D(0), \cdots, D(k), \cdots, D(N_c-1)]^T = \mathbf{Fd}$ and $\mathbf{W}_m = \mathrm{diag}[W_m(0), \cdots, W_m(k), \cdots, W_m(N_c-1)]$ is the MRT-FDE weight matrix associated with the mth antenna. $W_m(k)$ is given by

$$W_m(k) = \left(\frac{1}{N_c} \sum_{m'=0}^{N_t-1} \sum_{k'=0}^{N_c-1} \left| H_{m'}(k') \right|^2 \right)^{-\frac{1}{2}} H_m^*(k), \quad (20)$$

where $\{H_m(k); k = 0 \sim N_c - 1\}$ is the discrete Fourier transform of the channel impulse response $\{h_m(\tau); \tau = 0 \sim N_c - 1\}$.

The received signal at an MT can be expressed as

$$\begin{aligned}\mathbf{r} &= [r(0), \cdots, r(t), \cdots, r(N_c-1)]^T \\ &= \sqrt{\frac{2E_s}{T_s}} \mathbf{hs} + \mathbf{n}\end{aligned}, \quad (21)$$

where $\mathbf{h} = [\mathbf{h}_0, \cdots, \mathbf{h}_m, \cdots, \mathbf{h}_{N_t-1}]$ is the extended channel impulse response matrix of size $N_c \times (N_t N_c)$ and $\mathbf{n} = [n(0), \cdots, n(t), \cdots, n(N_c-1)]^T$ is the noise vector. Assuming a symbol-spaced L-path fading channel, $\mathbf{h}_m$ associated with the mth antenna is given as

$$\mathbf{h}_m = \begin{bmatrix} h_{m,0} & & & & h_{m,L-1} & \cdots & h_{m,1} \\ h_{m,1} & \ddots & & & & \ddots & \vdots \\ \vdots & \ddots & h_{m,0} & & \mathbf{0} & & h_{m,L-1} \\ h_{m,L-1} & & h_{m,1} & \ddots & & & \\ & \ddots & \vdots & \ddots & \ddots & & \\ & & h_{m,L-1} & & h_{m,0} & & \\ & & & \ddots & h_{m,1} & \ddots & \\ \mathbf{0} & & & \ddots & \vdots & \ddots & h_{m,0} \end{bmatrix}. \quad (22)$$

The frequency-domain representation $\mathbf{R}$ of the received signal block is given as

$$\mathbf{R} = \mathbf{Fr} = \sqrt{\frac{2E_s}{T_s}} \left(\sum_{m=0}^{N_t-1} \mathbf{H}_m \mathbf{W}_m \right) \mathbf{Fd} + \mathbf{N}, \quad (23)$$

where $\mathbf{H}_m = \mathbf{F}\mathbf{h}_m\mathbf{F}^H$ is the channel matrix of size $N_c \times N_c$ and $\mathbf{N} = \mathbf{Fn}$. $\mathbf{H}_m$ is diagonal and is given by

$$\mathbf{H}_m = \mathbf{F}\mathbf{h}_m\mathbf{F}^{\mathrm{H}} = \begin{bmatrix} H_m(0) & & & \mathbf{0} \\ & \ddots & & \\ & & H_m(k) & \\ \mathbf{0} & & & \ddots \\ & & & H_m(N_c-1) \end{bmatrix}. \quad (24)$$

MRT-FDE maximizes the received SNR at each frequency k, but enhances the ISI in the case of SC transmissions. Therefore, the ISI cancellation is necessary in the signal detection.

Similar to Eq. (8), the channel capacity C of SC DAN using MRT-FDE is given, from Eq. (23), as

$$C = \frac{1}{N_c}\log_2 \det\left(\mathbf{I} + \frac{E_s}{N_0}\left(\sum_{m=0}^{N_t-1}\mathbf{H}_m\mathbf{W}_m\right)\left(\sum_{m=0}^{N_t-1}\mathbf{H}_m\mathbf{W}_m\right)^H\right)$$
$$= \frac{1}{N_c}\sum_{k=0}^{N_c-1}\log_2\left(1 + \frac{E_s}{N_0}\frac{\left(\sum_{m=0}^{N_t-1}|H_m(k)|^2\right)^2}{\frac{1}{N_c}\sum_{m=0}^{N_t-1}\sum_{k'=0}^{N_c-1}|H_m(k')|^2}\right). \quad (25)$$

The channel capacity changes due to the frequency-selective fading, shadowing loss, and distant-dependent path loss according to the movement of an MT. The channel capacity distribution of SC MRT-FDE is plotted in Fig. 12. MRT-FDE can significantly increase the channel capacity. The use of around 5 antennas provides a sufficient improvement.

Another approach is the use of distributed antennas as relay nodes. Multiple relay nodes close to an MT cooperatively relay the signal transmitted from the MT to a BS. Multiple relay nodes can perform the antenna beam forming or MRT-FDE to improve the SC signal transmission performance. Note that in the case of OFDM, adaptive subcarrier allocation over multiple 2-hop routes constructed by relay nodes can be introduced to take advantage the frequency and space diversity [27].

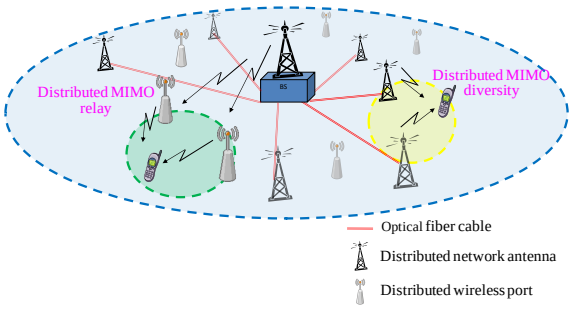

Fig. 10 Distributed antenna network.

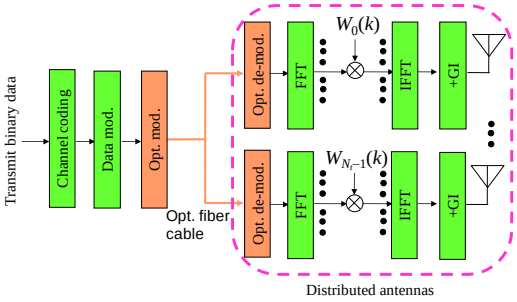

Fig. 11 DAN downlink using SC MRT-FDE.

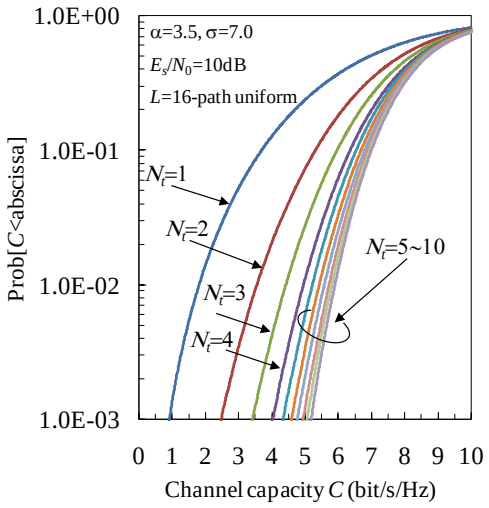

Fig. 12 Channel capacity distribution of distributed antenna diversity using SC MRT-FDE.

VII. CONCLUSIONS

This article introduced the recent advances in FDE and DAN for the broadband SC signal transmissions. To realize the high quality broadband SC signal transmissions, there are two crucial issues to overcome: the channel frequency-selectivity and the power loss due to the shadowing and distance-dependant path losses. The frequency-domain block signal detection that incorporates the idea of MIMO signal detection into FDE to effectively suppress the ISI was introduced. Also introduced was the oversampling one-tap MMSE-FDE that can mitigate the problem arising from the timing offset between the transmitter and receiver. Finally, DAN that can exploit the shadowing and path losses was presented. There remain a lot of interesting research topics before the realization of the broadband SC wireless communication systems.

REFERENCES

[1] Y. Kim, B. J. Jeong, J. Chung, C.-S. Hwang, J. S. Ryu, K.-H. Kim, and Y. J. Kim, "Beyond 3G; vision, requirements, and enabling technologies," IEEE Commun. Mag., Vol. 41, No. 3, pp. 120-124, Mar. 2003.

[2] J. G. Proakis, *Digital communications*, 4th edition, McGraw-Hill, 2001.

[3] D. Falconer, S. L. Ariyavistakul, A. Benyamin-Seeyar, and B. Eidson, "Frequency domain equalization for single-carrier broadband wireless systems," IEEE Commun. Mag., Vol. 40, pp. 58-66, Apr. 2002.

[4] A. S. Madhukumar, F. Chin, Y.-C. Liang, and K. Yang, "Single-carrier cyclic prefix-assisted CDMA system with frequency domain

equalization for high data rate transmission," EURASIP Journal on Wireless Communications and Networking, Vol. 2004, No. 1, pp. 149-160, Aug. 2004.

[5] F. Adachi, D. Garg, S. Takaoka, and K. Takeda, "Broadband CDMA techniques," IEEE Wireless Commun. Mag., Vol. 12, No. 2, pp. 8-18, Apr. 2005.

[6] F. Adachi, K. Takeda, and H. Tomeba, "Frequency-domain equalization for broadband single-carrier multiple access," IEICE Trans. Commun., Vol.E92-B, No. 05, pp. 1441-1456, May 2009.

[7] T. Yamamoto, K. Takeda, and F. Adachi, "A study of frequency-domain signal detection for single-carrier transmission," 2009 IEEE 70th Vehicular Technology Conference (VTC2009-Fall), Anchorage, Alaska, USA, 20–23 Sept. 2009.

[8] S. Liu, Z. He, and W. Wu, "Transmit diversity method with user's power constraint for distributed antenna system," Proc. 2nd International Symposium on Wireless Pervasive Computing (ISWPC'07), 5-7 Feb. 2007.

[9] A. A. M. Saleh, A. J. Rustako, and R. S. Roman, "Distributed antennas for indoor radio communications," IEEE Trans. Commun., Vol. 35, No. 12, pp.1245-1251, Dec. 1987.

[10] M. V. Clark, T. M. Willes III, L. J. Greenstein, A. J. Rustako, Jr, V. Erceg, and R. S. Roman, "Distributed versus centralized antenna arrays in broadband wireless networks," Proc. IEEE Veh. Technol. Conf. (VTC2001-Spring), pp. 33-37, May 2001.

[11] L. Dai, S. Zho, and Y. Yao, "Capacity analysis in CDMA distributed antenna systems," IEEE Trans. Wireless Commun., Vol. 4, No. 6, pp. 2613-2620, Nov. 2006.

[12] W. Choi, "Downlink performance and capacity of distributed antenna systems in a multicell environment," IEEE Trans. Wireless Commun., Vol. 6, No. 1, pp. 69-73, Jan. 2007.

[13] H. Matsuda, H. Tomeba, and F. Adachi, "Channel capacity of distributed antenna system using maximal ratio transmission," The 5th IEEE VTS Asia Pacific Wireless Communications Symposium (APWCS2008), Sendai, Japan, 21-22 Aug. 2008.

[14] T. S. Rappaport, *Wireless communications*, Prentice Hall, 1996.

[15] J. Louveaux, L. Vandendorpe, and T. Sartenaer, "Cyclic prefixed single carrier and multicarrier transmission: bit rate comparison," IEEE Commun., Lett., Vol. 7, No. 4 pp. 180-182, Apr. 2003.

[16] G. J. Foschini and M. J. Gans, "On limits of wireless communications in a fading environment when using multiple antennas," Wireless Personal Commun., Vol. 6, No. 3, pp. 311-335, Mar. 1998.

[17] H. Bolcskei, D. Gesbert, and A. J. Paulraj, "On the capacity of OFDM-based spatial multiplexing systems," IEEE Trans. Commun., Vol. 50, No. 2, pp. 225-234, Feb. 2002.

[18] P. W. Wolniansky, G. J. Foschini, G. D. Golden, and R. A. Valenzuela, "V-BLAST: an architecture for realizing very high data rates over the rich-scattering wireless channel," Proc. 1998 URSI International Symposium on Signals, Systems, and Electronics (ISSSE'98), pp.295-300, Pisa, Italy, 29 Sept.-2 Oct. 1998.

[19] L. J. Kim and J. Yue, "Joint channel estimation and data detection algorithms for MIMO-OFDM systems," Proc. Thirty-Sixth Asilomar Conference on Signals, System and Computers, pp. 1857-1861, Nov. 2002.

[20] R. Bohnke and K. Kammeyer, "SINR analysis for V-BLAST with ordered MMSE-SIC detection," Proc. International Wireless Communications and Mobile Computing Conference, pp. 623-628, July 2006.

[21] C. Shen, H. Zhuang, L. Dai, S. Zhou, and Y. Yao, "Performance improvement of V-BLAST through an iterative approach," Proc. IEEE Personal, Indoor and Mobile Radio Communications Symposium (PIMRC'03), Vol. 3, pp. 2553-2557, Sept. 2003.

[22] A. Nakajima and F. Adachi, "Throughput performance of iterative frequency-domain SIC with 2D MMSE-FDE for SC-MIMO multiplexing," Proc. IEEE Veh. Technol. Conf. (VTC'06-Fall), pp.25-28, Montreal, Quebec, Canada, Sept. 2006.

[23] K. Takeda and F. Adachi, "HARQ throughput performance of multicode DS-CMDA with MMSE turbo equalization," Proc. IEEE Veh. Technol. Conf. (VTC'01-Spring), pp.1603-1607, Ireland, Apr. 2007.

[24] J. B. Anderson and S. Mohan, "Sequential coding algorithms: A suever and cost analusis," IEEE Trans. on Commun., Vol. 32, pp. 169-176, Feb. 1984.

[25] T. Obara, K. Takeda, and F. ADachi, "Oversampling frequency-domain equalization for single-carrier transmission in the presence of timing fffset," The 6th IEEE VTS Asia Pacific Wireless Communications Symposium (APWCS'09), Seoul, Korea, Aug. 20~21, 2009.

[26] J. K. Cavers, "Single-user and multiuser adaptive maximal ratio transmission for Rayleigh channels," IEEE Trans. Veh. Tech., Vol. 49, No. 6, pp. 2043-2050, Nov. 2000.

[27] H. Ishida, E. Kudoh, and F. Adachi, "Channel capacity of parallel relaying 2-hop OFDMA virtual cellular network," Proc. IEEE 70th Vehicular Technology Conference (VTC'09-Fall), Anchorage, Alaska, USA, 20–23 Sept. 2009..